ACS APPLIED MATERIALS & INTERFACES

Research Article

www.acsami.org

Photoinduced Charge Transfer within Polyaniline-Encapsulated Quantum Dots Decorated on Graphene

Kim Truc Nguyen,[†] Dehui Li,[‡] Parijat Borah,[†] Xing Ma,[§] Zhaona Liu,[§] Liangliang Zhu,[†] George Grüner,[⊥] Qihua Xiong,[‡,#] and Yanli Zhao*[,†,§]

[†]Division of Chemistry and Biological Chemistry, School of Physical and Mathematical Sciences, [‡]Division of Physics and Applied Physics, School of Physical and Mathematical Sciences, Nanyang Technological University, 21 Nanyang Link, Singapore 637371

[§]Materials Science and Engineering School, Nanyang Technological University, 50 Nanyang Avenue, Singapore 639798

[⊥]Department of Physics and Astronomy, University of California, Los Angeles, California 90095, United States

[#]Division of Microelectronics, School of Electrical and Electronic Engineering, Nanyang Technological University, Singapore 639798

Supporting Information

ABSTRACT: A new method to enhance the stability of quantum dots (QDs) in aqueous solution by encapsulating them with conducting polymer polyaniline was reported. The polyaniline-encapsulated QDs were then decorated onto graphene through $\pi-\pi$ interactions between graphene and conjugated polymer shell of QDs, forming stable polyaniline/QD/graphene hybrid. A testing electronic device was fabricated using the hybrid in order to investigate the photoinduced charge transfer between graphene and encapsulated QDs within the hybrid. The charge transfer mechanism was explored through cyclic voltammetry and spectroscopic studies. The hybrid shows a clear response to the laser irradiation, presenting a great advantage for further applications in optoelectronic devices.

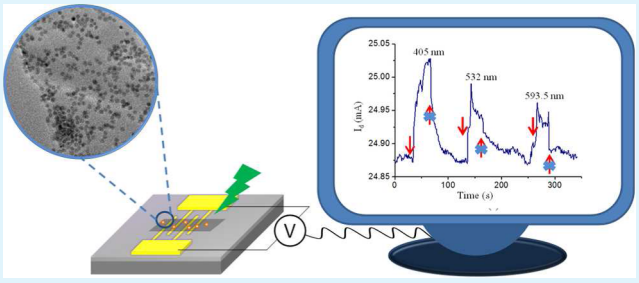

KEYWORDS: *charge transfer, graphene, quantum dots, photovoltaic devices, polyaniline*

INTRODUCTION

Responsive hybrid materials with nanoscale components have been at the forefront of scientific research. One particular area involves hybrid materials where one component is electrically conducting and other components display well-defined functionality, and thus the hybrid materials could respond to the environment. The interface between the different components underlies most of the phenomena that have been investigated and exploited for applications in optoelectronics, renewable energy, biotechnology, etc.[1−3] Mechanically robust interface that allows charge transfer across the components is essential for the applications above-mentioned. However, such an interface that obeys these requirements is actually not straightforward to achieve, and a simple mixture of the components usually cannot lead to the required intimate contact. Thus, new strategies for developing such hybrid materials are needed.

As a promising application, responsive hybrid materials for photovoltaic devices are currently drawing immense attention on account of the scarcity of fossil fuel. Thus far, the use of metal oxide, semimetal nanocrystals, or organic compounds as the optical absorption components in those photovoltaic devices has been widely explored, and some photovoltaic devices have been employed as a source of green energy.[4−6] These systems, however, still have some limitations such as low efficiency of organic solar cell,[7] as well as short lifetime of some metal oxides and semimetal nanocrystals due to their unavoidable oxidation under ambient conditions.[8] Electron generated from semimetal nanocrystals has been reported to provide a high efficiency than that generated from organic dyes.[9−13] Hence, it is important to develop new types of hybrid materials using semimetal nanocrystals, which can efficiently convert light into electricity, and at the same time, remain stable under ambient conditions.

Graphene-carbon-based two-dimensional (2D) system with atom thickness - has attracted considerable interests in recent years on account of its unique structure and properties.[14,15] In particular, single graphene sheet without defect and oxygen components have been reported to present superconductive property,[16,17] which is due to the π electron cloud surrounding the graphene surface.[18] In addition to its fascinating electronic properties, single-layered graphene and few-layered graphene have an optical transparency about 83 to 93%.[19] In essence, these properties make graphene a promising candidate for various applications in nanoelectronics.[20−22] Inspired by these encouraging findings, herein, we report a new strategy to

Received: June 5, 2013
Accepted: July 15, 2013
Published: July 15, 2013

prepare graphene/quantum dot (QD) hybrid by synergistically combining intrinsic electronic properties of graphene and QDs.

In this work, CdSe QDs were used as the light absorption cores in order to generate electrons, whereas graphene with the 2D morphology was employed as the electron acceptor. At first, CdSe was encapsulated by a conducting polymer—polyaniline, which serves as a bridge connecting between CdSe and graphene for the electron transport. In addition, the polymer encapsulation offers two important features: (a) the protection of CdSe from fast degradation, and (b) the immobilization of CdSe onto graphene through the $\pi-\pi$ interaction. The polymer encapsulation of QDs in aqueous solution undergoes two simultaneous processes, i.e., phase transfer and ligand exchange. The proposed mechanism for these processes is shown in Scheme 1. In the preparation of the hybrid, the $\pi-\pi$ stacking

Scheme 1. Illustration for the Ligand and Phase Exchange Process Followed by the Polymerization of Aniline on the Surface of CdSe QDs

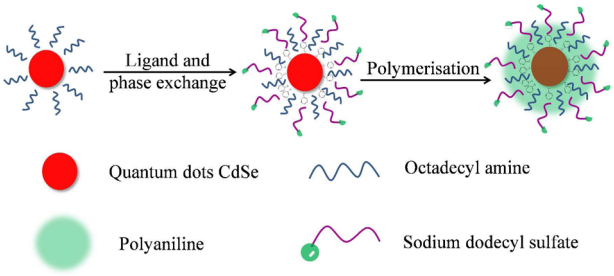

interactions between the polyaniline shell and graphene leads to relatively stable hybrid, which are beneficial to the measurements of the photoinduced charge transfer. Thus, present research provides a novel approach for making stable graphene/QD hybrids toward functional applications.

EXPERIMENTAL SECTION

Synthesis of Polyaniline/QD/Graphene Hybrid. *Materials.* Aniline (99%, Alfa Aesar) was distilled before use and stored at 4 °C. CdSe QDs (5 mg mL^{-1} in toluene, stabilized by octadecyl amine (ODA) ligand) were purchased from Nanomaterials and Nanofabrication Laboratories (NN-Laboratories, LLC). Ammonium persulfate (98%, Alfa Aesar), chloroform (99%, Sigma), dimethylformamide (DMF) (99.5%, Merck), graphene nanopowder (C, 6–8 nm, SS NANO), HCl (38%, Sigma), and sodium dodecyl sulfate (SDS) (99%, Alfa Aesar) were used as received. All solutions were prepared using ultrapure water (resistance >18 MΩ), which was obtained from a Millipore Simplicity 185 system. Formvar stabilized with carbon 300 meshes, high-resolution lacey Formvar/carbon, and 200 meshes copper grids were purchased from Beijing XXBR Technology Co. Silicon wafer with 100 mm in diameter and 500 μm in thickness purchased from University Wafer was cut into pieces of 0.5 × 0.5 cm, which was used as solid substrates for SEM samples.

Instruments. Transmission electron microscopy (TEM) images were collected on a JEM-1400 (JEOL) operated at 100–120 kV. High-resolution transmission electron microscopy (HR TEM) images were collected on JEM-2010 (JEOL) at 200 kV. Scanning electron microscopy (SEM) images were collected on a Field emission JSM-6700F (JEOL) operated at 10 kV. Emission spectra were recorded on RF-5301 PC spectrofluorophotometer (Shimadzu) with 1.0 cm path length cell, while absorption spectra were recorded on UV-3600 UV–vis–NIR spectrophotometer (Shimadzu). Ultra sonication processes were carried out with VCX 130 sonicator (SONICS) under the power of 130 kW at the frequency of 35 kHz. X-ray photoelectron spectroscopy (XPS) was carried out on SPECS HAS 3500 Plus spectrometer using Mg X-ray source.

Synthesis of Polyaniline Modified CdSe (QD@PANI). The CdSe solution in chloroform (18.92 nM, 0.3 mL) was added into a vial containing a solution of aniline (2 mM, 1.5 mL) and SDS (40 mM, 300 μL) under vigorous stirring. The solution was heated at 65 °C for half hour to evaporate completely chloroform. After cooling down to room temperature, the solution was sonicated for 5 s followed by addition of acidic $(NH_4)_2S_2O_8$ solution (2 mM in 10 mM HCl, 1.5 mL). After vortexing for 10 s, the solution was incubated at room temperature overnight to ensure the complete polymerization. The final solution was centrifuged at 10 k rpm for 10 min and the modified QDs were redispersed in SDS (3 mL, 3.6 mM). QD@PANI was characterized with electron microscopy and absorption spectroscopy.

Preparation of Single-Layer Graphene. Graphene nanopowder (1 mg) as purchased was dispersed in DMF (3 mL). The dispersion was sonicated with ultra sonicator probe for 4 h in order to break the $\pi-\pi$ interaction between layers in graphene powder. After sonication, the solution was centrifuged at 2000 rounds per minute (rpm) for 5 min. Then, the supernatant was extracted and subjected to centrifugation at 4000 rpm for 5 min. This process was repeated at increasing centrifugation speeds of 8000, 10000, and 13500 rpm. Finally, clear blackish supernatant after centrifugation at 13500 rpm was used as the source of single layer graphene for further studies. Single-layer graphene in supernatant was characterized by SEM, TEM, and selected area electron diffraction (SAED).

Hybrid of Single-Layer Graphene Coated with Encapsulated QDs (QD@PANI-G). Polyaniline encapsulated QD solution (0.5 mL) was concentrated by centrifugation at 10 k rpm to a volume of 10 μL. This concentrated solution was added into the equal volume of single-layer graphene that was prepared as described above. The mixture solution was sonicated by normal sonicating bath for around 10 min to ensure homogeneous distribution of encapsulated QDs on graphene.

Device Fabrication for Light-Induced Charge Transfer within the Hybrid. *Materials.* Silicon wafer (P(100), 1–100 ohm cm) with 100 mm in diameter and 500 μm in thickness, and 300 nm of silicon oxide layer on polished side purchased from University Wafer was used as the solid substrate for the device fabrication. Gold pellets (99.99%, MOS group Pte Ltd.) were used as the gold source for the electrode fabrication. Poly(methyl methacrylate) 4 (PMMA4) and methyl methacrylate 8.5 (MMA 8.5) purchased from Micro Chem were used as high-resolution positive resist for direct write e-beam. Methyl isobutyl ketone (MIBK) (99.5%, Sigma), isopropanol (IPA) (99.7%, Sigma), and acetone (99.5%, P.P Chemicals) were used as washing solvents during the fabrication process.

Instruments. E-beam lithography was carried out on a field-emission JSM-7001F (JEOL) operated at 30 kV. Copolymer resist was spin-coated by Specialty Coating Systems spin coater P6700. I_d-V_d characteristic curve was measured on Lakeshore probe station. E-beam metal deposition was carried out in Nanyang NanoFabrication Center, Nanyang Technological University.

Device Fabrication for Light-Induced Charge Transfer within the Hybrid. Silicon wafer with 300 nm of silicon oxide layer (SiO_2/Si) was cut into small pieces with dimension of 0.5 × 0.5 cm^2. The wafers were sonicated in acetone solution and then in isopropanol solution for 15 min each. The wafers were washed again with ultrapure water before blow-drying by nitrogen gas. Methyl methacrylate (MMA) was spin-coated on the cleaned wafer at 4000 rpm, after which, PMMA4 was spin-coated on top of the MMA layer under the same speed. E-beam lithography was drawn on the resist-coated wafer by following a predesigned pattern generated by Nano Pattern Generating System. The patterned wafers were washed in solution of MIBK/IPA (1:3 volume ratio) for 90 s. After the E-beam metal deposition with Ti (2 nm) and Au (30 nm), the wafers were washed in boiling acetone to lift off all the resist and metal deposition that were not in direct contact with the SiO_2/Si surface. Finally, the QD@PANI-G hybrid was deposited on top of the wafer by drop casting method, and the electrical measurements were performed at room temperature (T = 28 °C) under ambient conditions. The whole fabrication process was illustrated in Scheme 2.

Scheme 2. Illustration for the Device Fabrication Using QD@PANI-G Hybrid

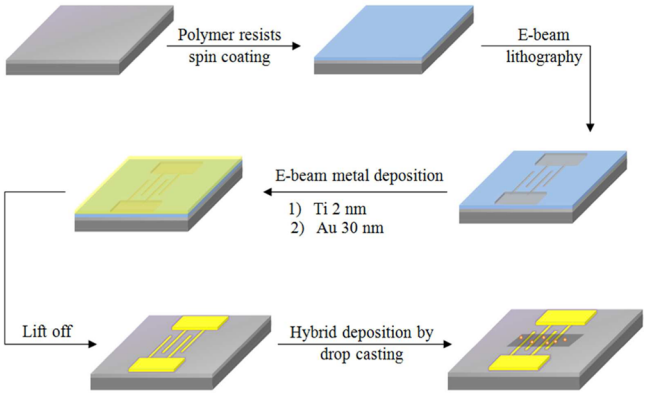

RESULTS AND DISCUSSION

After introducing aniline and SDS in H_2O into the stock solution of QDs in $CHCl_3$, the ligand exchange process between aniline and octadecylamine (ODA) that was already presented as the stabilizing agent for QDs occurred on the surface of QDs. Alongside this process, the phase transfer of QDs also took place from $CHCl_3$ to H_2O medium. It should be noted that the role of SDS is to provide negative charges to the QD surface, which stabilize the encapsulated QDs in aqueous solution via the charge−charge repulsion between QDs. The ligand exchange and the phase exchange process were also carried out in the absence of SDS in order to validate our proposed mechanism. The absence of SDS led to large aggregation of QDs, which was observed from TEM image as shown in Figure 1b.

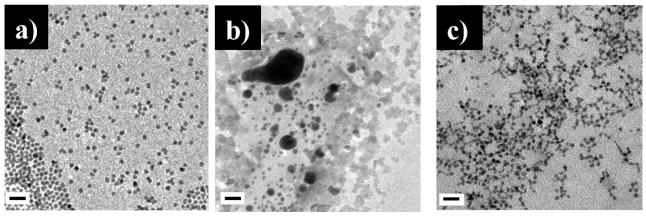

Figure 1. TEM images of (a) CdSe QDs in $CHCl_3$ before the ligand and phase exchange processes, (b) aggregation of QDs after ligand exchange process without the SDS surfactant, and (c) QD@PANI in SDS solution (3.6 mM). Scale bars are 20 nm.

After the ligand exchange process, aniline was polymerized in the presence of $(NH_4)_2S_2O_8$, resulting in complete encapsulation of QDs. During this process, aniline was oxidized to its emeraldine base form that can be inferred from its characteristic green color as shown in Figure 2 and its absorption peaks at 430 and 770 nm (Figure S1 in the Supporting Information).[23] The purified polyaniline-encapsulated QDs (QD@PANI) dispersed in SDS solution (3.6 mM) show an absorption peak at 633 nm (Figure S1 in the Supporting Information), whereas nonencapsulated QDs show corresponding peak at 618 nm (Figure S1 in the Supporting Information). This significant peak shifting in the absorption spectra provides clear evidence for the surface encapsulation of QDs. QD@PANI was also characterized by TEM as shown in Figure 1c.

The experimental conditions we used in the preparation of QD@PANI are the optimized conditions for obtaining well-

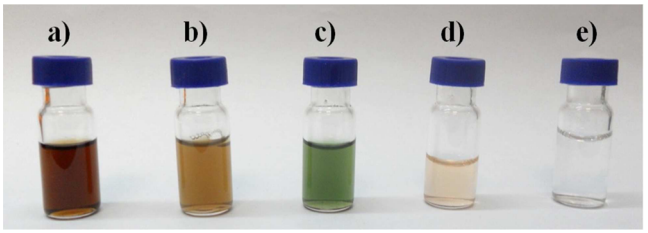

Figure 2. Photo images show clearly the color changes at each stage of the modification processes. (a) CdSe QDs in $CHCl_3$ before the ligand and phase exchange processes, (b) CdSe QDs after the ligand and phase exchange processes, (c) QD@PANI before purifications, (d) QD@PANI after purifications in SDS solution (3.6 mM), and (e) pure water for color comparison.

dispersed and uniform QD@PANI hybrid. We also tried controlling the thickness/content of polyaniline shell on QDs, as the thickness/content may influence the charge transfer from QD@PANI to graphene. When increasing the amount of the aniline in the synthesis process, the results we obtained were not good to carry out the experiments for determining the thickness/content effect on the photocurrent. We observed significant aggregation of QDs and the formation of free polyaniline in a needlelike shape which links QDs together.

QD@PANI exhibits unprecedented stability in aqueous solution under ambient conditions without any aggregation or color change for over three months. On the contrary, the non- encapsulated QDs undergo rapid dissolution in aqueous medium within a few hours due to the oxidation of CdSe into Cd and Se species.[8] This unwanted oxidation was circumvented by the polymer encapsulation that endows the dramatic stability to QDs. Moreover, this conducting polymer plays an important role in the charge transfer from the electron donor (QDs) to the electron acceptor (graphene), which will be discussed later.

Single layered graphene with a uniform dimension was obtained through a process as described in the Experimental Section, and it was well-characterized by SEM, TEM, and SAED (Figure S2 in the Supporting Information). One of the crucial factors that suppresses the electronic properties of graphene is its unwanted oxygen content.[12] Therefore, the oxygen content on graphene was investigated by XPS, showing a negligible amount of oxygen (3%) (Figure S3 in the Supporting Information).

The hybrid of QD@PANI coated graphene (QD@PANI-G) was prepared simply through mixing concentrated aqueous solution of QD@PANI with graphene dispersion. The $\pi-\pi$ interaction between graphene and polyaniline layer on QDs was believed to be the driving force for the immobilization of QD@PANI on graphene. To confirm the crucial role of the polyaniline layer for the immobilization, we carried out controlled experiments by using gold nanoparticles (AuNPs) as replica of QDs. For this purpose, citrate-capped AuNPs with diameter of 15 nm (Figure S4a in the Supporting Information) were synthesized through Frens' method.[24] Then, the graphene hybrids coated by AuNPs with and without the polyaniline layer were investigated by TEM, clearly showing that AuNPs cannot be immobilized on the graphene sheet (Figure S4b in the Supporting Information) in the absence of the polyaniline shell. However, both AuNPs and QDs can be homogeneously distributed on the graphene sheet in the presence of the polyaniline shell as shown in images a and b in Figure 3, respectively. Furthermore, homogeneous distribution of QD@PANI on graphene could reduce the thickness of QD film,

dx.doi.org/10.1021/am402182z | ACS Appl. Mater. Interfaces 2013, 5, 8105−8110

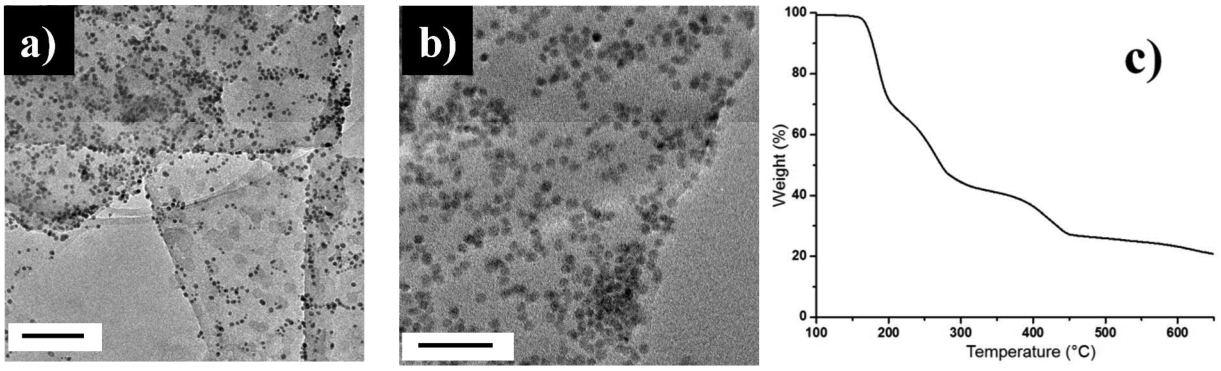

Figure 3. TEM images of (a) graphene coated with polyaniline-modified AuNPs, scale bar is 100 nm, and (b) graphene coated with polyaniline-encapsulated QDs (QD@PANI-G), scale bar is 50 nm. (c) TGA graph of QD@PANI-G.

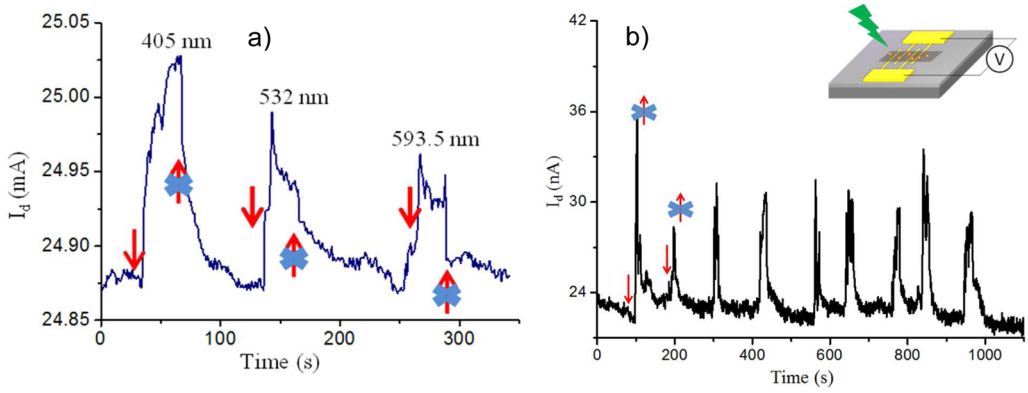

Figure 4. (a) Current-versus-time curve of the hybrid-based device under irradiation of different laser sources (405, 532, and 593.5 nm, respectively) with an irradiation time interval of 30 s. The red arrows indicate the starting point of laser irradiation, where red arrows with the *x* marks indicate the stopping point of laser irradiation. (b) Current-versus-time curve of the hybrid-based device under laser irradiation of 532 nm with irradiation time interval of 30 s for 9 cycles. The inset shows the device scheme for the measurements.

leading to enhanced charge separation and effective loading of QDs on graphene.[25−27]

The content of polyaniline in the hybrid was determined by thermogravimetric analysis (TGA). Pure polyaniline showed the degradation temperature at 274 °C (Figure S5 in the Supporting Information), and the content of polyaniline in QD@PANI-G was determined to be 25 wt % according to the weight loss of the hybrid at this temperature (Figure 3c).

In order to evaluate the charge transfer efficacy within QD@PANI-G hybrid, testing devices were fabricated on the SiO_2/Si substrate with a fixed dimension (Figure S6 in the Supporting Information). The device fabrication process is illustrated in Scheme 2 and the fabrication procedure is shown in the experimental section. The I_d−V_d curves (current versus voltage curves) for testing devices were recorded on the Lakeshore probe station scanning voltage from −1 to 1 V with an increasing step of 0.01 V. Perfect linear and symmetric I_d−V_d curves were observed for QD@PANI-G-based devices, indicating the presence of Ohmic contact.[28]

The I_d-V_d measurements were further carried out using QD@PANI-G-based devices in the dark as well as under 532 nm laser irradiation (Figure S7 in the Supporting Information). The device shows 5.9% decreased resistance under the irradiation as compared with that in the dark, which indicates more current flows between source-drain electrodes. When laser light was shined directly onto the device, the current between the source-drain electrodes immediately rose up. A significant decrease of current flow was observed when the light was removed. The light induced property was also investigated with different laser wavelengths at same intensity of 1 W m^{-2}. When lasers with different wavelengths of 405, 532, and 593.5 nm were used, corresponding current flows were recorded as 156, 117, and 92 μA, respectively (Figure 4a). These observations indicate an obvious decrease in the current flow upon increasing the corresponding irradiation wavelength. The main reason for the decrease of the current flows upon increasing the laser wavelength is that the absorption intensity of QDs was decreased in the range from 400 to 600 nm (Figure S8 in the Supporting Information), and thus the electron generated from excited QDs was also reduced according to the decreased absorption intensity. The changes in resistance of the QD@PANI-G-based device in response to light with varying wavelengths and constant intensity are shown in Figure S8 of the Supporting Information, overlaid with the absorption spectrum of QDs recorded in $CHCl_3$ solution at 25 °C. The clear correlation between the magnitude of the changes in photocurrent of the device and the absorption spectrum of QDs provides direct evidence to indicate that the light-induced change of the hybrid is coupled to the charge-transfer process.[29−37] Under the same absorption intensity as well as laser wavelength, the device response was not significantly changed after 9 cycles, indicating good stability of the current device (Figure 4b). Notably, similar results were obtained when the measurements were carried out using QD@PANI-G that was incubated in aqueous solution for 3 months, providing

further evidence for the stability of polymer-coated QDs on graphene.

A mechanism for the charge transfer within the QD@PANI-G hybrid was proposed, where the electrons generated from QDs upon the absorption of the light energy are transferred to graphene through the conducting polyaniline shell.[38] The validity of the hypothesis is totally dependent on the HOMO and LUMO levels of respective components, namely CdSe QDs, polyaniline shell, and graphene. CdSe with the diameter size of 5−6 nm was reported to have the energy levels of HOMO and LUMO as −5.36 and −3.32 eV, respectively.[39] The graphene surface energy level is at −4.5 eV.[40] Polyaniline was reported to have three different oxidation states, i.e., leucoemeraldine, emeraldine, and (per)nigraniline.[41] To achieve a firm conclusion, we carried out the cyclic voltammetry (CV) experiment to calculate the exact HOMO and LUMO levels for polyaniline in QD@PANI-G. CV curves for both polyaniline and ferrocence were shown in Figures S9 and S10 of the Supporting Information. HOMO and LUMO energy levels (E_{HOMO} and E_{LUMO}) of polyaniline were calculated through the following equations using ferrocence as the reference potential (E_{ref}).[42]

$$E_{HOMO} = (-4.8 + E_{ref} - E_{ox})\ \text{eV}$$

$$E_{LUMO} = (-4.8 + E_{ref} - E_{red})\ \text{eV}$$

Where, $E_{ref} = (E_{ox} + E_{red})/2$, and E_{ox} and E_{red} refer to the oxidation and reduction potentials, respectively.

On the basis of these equations, the energy levels of HOMO and LUMO for polyaniline were calculated to −4.75 and −3.95 eV, respectively. These energy levels lie between HOMO−LUMO of CdSe and graphene energy levels. Thus, the polyaniline shell could facilitate the charge transfer process between CdSe QDs and graphene, which validates our hypothesis. A diagram illustrated the charge transfer process within the hybrid from QDs to graphene is shown in Figure 5.

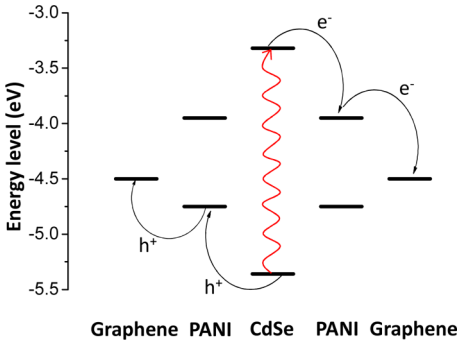

Figure 5. Illustration for the charge transfer process within the hybrid. Light excites CdSe electron to its LUMO, and it was then transferred to LUMO of surrounding polyaniline followed by transferring to graphene. Meanwhile, holes were transferred from CdSe LUMO to polyaniline LUMO and then to graphene.

Moreover, the photoresponse of QDs without the polyaniline shell on graphene layer was not observed from our experiment (Figure S11 in the Supporting Information). This observation hence confirms the important role of the polyaniline shell during the charge transfer process. Without coating of the polyaniline shell, monodispersed CdSe nanocrystals were stabilized by octadecylamine that blocks the essential pathway of the charge transfer from CdSe to graphene layer. Similar blocking effect was reported using other nanocrystals such as PdS on graphene layer.[43]

CONCLUSIONS

In summary, we have successfully synthesized polyaniline-encapsulated CdSe quantum dots that show tremendous stability in aqueous solution under ambient conditions. Then, a novel hybrid material has been fabricated by the immobilization of polyaniline encapsulated quantum dots onto the graphene surface through the $\pi-\pi$ interactions. The light-induced charge transfer between polyaniline encapsulated quantum dots and graphene within this hybrid material has been successfully evaluated, and a mechanism responsible for this charge transfer process has been established. The improved photovoltaic property of the hybrid in response to light is expected to have a great application potential for the fabrication of optoelectronic devices in the near future.

ASSOCIATED CONTENT

Supporting Information

Additional absorption spectra, SEM and TEM images, XPS spectra, thermogravimetric analysis, I_d-V_d curves, cyclic voltammogram curves, and current-versus-time curves. This material is available free of charge via the Internet at http://pubs.acs.org.

AUTHOR INFORMATION

Corresponding Author

*E-mail: zhaoyanli@ntu.edu.sg.

Notes

The authors declare no competing financial interest.

ACKNOWLEDGMENTS

We thank the Singapore National Research Foundation Fellowships (NRF2009NRF-RF001-015 and NRF-RF2009-06), the Singapore National Research Foundation CREATE program — Singapore Peking University Research Centre for a Sustainable Low-Carbon Future, and the Centre of Excellence for Silicon Technologies (A*Star SERC no.: 112 351 0003) for financial support.

REFERENCES

(1) Georgakilas, V.; Otyepka, M.; Bourlinos, A. B.; Chandra, V.; Kim, N.; Kemp, K. C.; Hobza, P.; Zboril, R.; Kim, K. S. *Chem. Rev.* **2012**, *112*, 6156−6214.
(2) Zhao, Y. L.; Grüner, G. *J. Mater. Chem.* **2012**, *22*, 24983−24991.
(3) Chen, J.; Xu, F.; Wu, J.; Qasim, K.; Zhou, Y.; Lei, W.; Sun, L.; Zhang, Y. *Nanoscale* **2012**, *4*, 441−443.
(4) Shen, G.; Chen, P.-C.; Ryu, K.; Zhou, C. *J. Mater. Chem.* **2009**, *19*, 828−839.
(5) Eritt, M.; May, C.; Leo, K.; Toerker, M.; Radehaus, C. *Thin Solid Films* **2010**, *518*, 3042−3045.
(6) Cao, W.; Zheng, Y.; Li, Z.; Wrzesniewski, E.; Hammond, W. T.; Xue, J. *Org. Electron.* **2012**, *13*, 2221−2228.
(7) Park, S. H.; Roy, A.; Beaupre, S.; Cho, S.; Coates, N.; Moon, J. S.; Moses, D.; Leclerc, M.; Lee, K.; Heeger, A. J. *Nat. Photon* **2009**, *3*, 297−302.
(8) Xi, L.; Lek, J. Y.; Liang, Y. N.; Boothroyd, C.; Zhou, W.; Yan, Q.; Hu, X.; Chiang, F. B. Y.; Lam, Y. M. *Nanotechnology* **2011**, *22*, 275706.
(9) Hu, L.; Zhao, Y. L.; Ryu, K.; Zhou, C.; Stoddart, J. F.; Grüner, G. *Adv. Mater.* **2008**, *20*, 939−946.
(10) Alivisatos, A. P.; Gur, I.; Fromer, N. A.; Chen, C. P.; Kanaras, A. G. *Nano Lett.* **2007**, *7*, 409−414.
(11) Kamat, P. V. *Acc. Chem. Res.* **2012**, *45*, 1906−1915.

(12) Kamat, P. V. *J. Phys. Chem. C* **2008**, *112*, 18737−18753.
(13) Loef, R.; Houtepen, A. J.; Talgorn, E.; Schoonman, J.; Goossens, A. *Nano Lett.* **2009**, *9*, 856−859.
(14) Novoselov, K. S.; Falko, V. I.; Colombo, L.; Gellert, P. R.; Schwab, M. G.; Kim, K. *Nature* **2012**, *490*, 192−200.
(15) Novoselov, K. S.; Geim, A. K.; Morozov, S. V.; Jiang, D.; Zhang, Y.; Dubonos, S. V.; Grigorieva, I. V.; Firsov, A. A. *Science* **2004**, *306*, 666−669.
(16) Lee, E. J. H.; Balasubramanian, K.; Weitz, R. T.; Burghard, M.; Kern, K. *Nat. Nanotechnol.* **2008**, *3*, 486−490.
(17) Jung, I.; Dikin, D. A.; Piner, R. D.; Ruoff, R. S. *Nano Lett.* **2008**, *8*, 4283−4287.
(18) Areshkin, D. A.; Gunlycke, D.; White, C. T. *Nano Lett.* **2007**, *7*, 204−210.
(19) Li, X.; Zhang, G.; Bai, X.; Sun, X.; Wang, X.; Wang, E.; Dai, H. *Nat. Nanotechnol.* **2008**, *3*, 538−542.
(20) Meyer, J. C.; Geim, A. K.; Katsnelson, M. I.; Novoselov, K. S.; Booth, T. J.; Roth, S. *Nature* **2007**, *446*, 60−63.
(21) Coleman, J. N.; Lotya, M.; O'Neill, A.; Bergin, S. D.; King, P. J.; Khan, U.; Young, K.; Gaucher, A.; De, S.; Smith, R. J.; Shvets, I. V.; Arora, S. K.; Stanton, G.; Kim, H.-Y.; Lee, K.; Kim, G. T.; Duesberg, G. S.; Hallam, T.; Boland, J. J.; Wang, J. J.; Donegan, J. F.; Grunlan, J. C.; Moriarty, G.; Shmeliov, A.; Nicholls, R. J.; Perkins, J. M.; Grieveson, E. M.; Theuwissen, K.; McComb, D. W.; Nellist, P. D.; Nicolosi, V. *Science* **2011**, *331*, 568−571.
(22) Yang, D.; Velamakanni, A.; Bozoklu, G.; Park, S.; Stoller, M.; Piner, R. D.; Stankovich, S.; Jung, I.; Field, D. A.; Ventrice, C. A., Jr; Ruoff, R. S. *Carbon* **2009**, *47*, 145−152.
(23) Xing, S.; Tan, L. H.; Yang, M.; Pan, M.; Lv, Y.; Tang, Q.; Yang, Y.; Chen, H. *J. Mater. Chem.* **2009**, *19*, 3286−3291.
(24) Frens, G. *Nat. Phys. Sci.* **1973**, *241*, 20−22.
(25) Lightcap, I. V.; Kamat, P. V. *J. Am. Chem. Soc.* **2012**, *134*, 7109−7116.
(26) Cao, A.; Liu, Z.; Chu, S.; Wu, M.; Ye, Z.; Cai, Z.; Chang, Y.; Wang, S.; Gong, Q.; Liu, Y. *Adv. Mater.* **2010**, *22*, 103−106.
(27) Wang, P.; Jiang, T.; Zhu, C.; Zhai, Y.; Wang, D.; Dong, S. *Nano Res* **2010**, *3*, 794−799.
(28) Venugopal, A.; Colombo, L.; Vogel, E. M. *Appl. Phys. Lett.* **2010**, *96*, 013512.
(29) Hecht, D. S.; Ramirez, R. J. A.; Briman, M.; Artukovic, E.; Chichak, K. S.; Stoddart, J. F.; Grüner, G. *Nano Lett.* **2006**, *6*, 2031−2036.
(30) Zhao, Y. L.; Hu, L.; Grüner, G.; Stoddart, J. F. *J. Am. Chem. Soc.* **2008**, *130*, 16996−17003.
(31) Kim, Y.; Shin, H.; Ko, Y.; Ahn, T.; Kwon, Y. *Nanoscale* **2013**, *5*, 1483−1488.
(32) Schubert, C.; Wielopolski, M.; Mewes, L.-H.; Rojas, G. M.; van der Pol, C.; Moss, K. C.; Bryce, M. R.; Moser, J. E.; Clark, T.; Guldi, D. M. *Chem.—Eur. J.* **2013**, *19*, 7575−7586.
(33) Guldi, D. M.; Rubén, D. C. *J. Phys. Chem. Lett.* **2013**, *4*, 1489−1501.
(34) Katrin, P.; Theodore, L.; Dimitra, D.; Georgios, C.; Georgios, L.; Axel, K.; Randy, P.; David, W. M.; Daniel, T. G.; Athanassios, G. C.; Guldi, D. M. *J. Phys. Chem. C* **2013**, *117*, 1647−1655.
(35) Rubén, D. C.; Jenny, M.; Wolfgang, B.; Norbert, J.; Guldi, D. M. *Adv. Mater.* **2013**, *25*, 2600−2605.
(36) Matthias, K.; Giovanni, B.; Giuseppe, B.; Vincenzo, B.; Guldi, D. M.; Tomás, T. *Chem. Sci.* **2013**, *4*, 2502−2511.
(37) Wolfgang, B.; Jenny, M.; Rubén, D. C.; Guldi, D. M.; Norbert, J. *Adv. Mater.* **2013**, *25*, 2314−2318.
(38) Knappenberger, K. L.; Wong, D. B.; Romanyuk, Y. E.; Leone, S. R. *Nano Lett.* **2007**, *7*, 3869−3874.
(39) Zhou, Y.; Eck, M.; Kruger, M. *Energy Environ. Sci.* **2010**, *3*, 1851−1864.
(40) He, M.; Jung, J.; Qiu, F.; Lin, Z. *J. Mater. Chem.* **2012**, *22*, 24254−24264.
(41) Feast, W. J.; Tsibouklis, J.; Pouwer, K. L.; Groenendaal, L.; Meijer, E. W. *Polymer* **1996**, *37*, 5017−5047.
(42) Zhu, R.; Wen, G.-A.; Feng, J.-C.; Chen, R.-F.; Zhao, L.; Yao, H.-P.; Fan, Q.-L.; Wei, W.; Peng, B.; Huang, W. *Macromol. Rapid Commun.* **2005**, *26*, 1729−1735.
(43) Zhang, D.; Gan, L.; Cao, Y.; Wang, Q.; Qi, L.; Guo, X. *Adv. Mater.* **2012**, *24*, 2715−2720.